Journal of Chromatography B, 878 (2010) 363–370

Contents lists available at ScienceDirect

Journal of Chromatography B

journal homepage: www.elsevier.com/locate/chromb

Metabolites of puerarin identified by liquid chromatography tandem mass spectrometry: Similar metabolic profiles in liver and intestine of rats

Cheng-Feng Luo [a], Mu Yuan [b], Min-Sheng Chen [a,*], Shi-Ming Liu [a], Hong Ji [b]

[a] The Second Affiliated Hospital of Guangzhou Medical College, Guangzhou Institute of Cardiovascular Disease, 250, Changgangdong Road, Guangzhou 510260, China
[b] Guangzhou Medical College, Guangzhou 510182, China

ARTICLE INFO

Article history:
Received 17 October 2009
Accepted 1 December 2009
Available online 5 December 2009

Keywords:
Puerarin
Metabolites
Liquid chromatography tandem mass spectrometry
Glucuronidation

ABSTRACT

Puerarin is a major active ingredient of Pueraria Radix. Puerarin may exert its medicinal functions in part via its metabolites. In this study, we identified these metabolites to better understand and elucidate puerarin's metabolic pathway. Puerarin was intravenously administered to rats and then metabolites in plasma samples were identified by rapid resolution liquid chromatography electrospray ionization-collision induced dissociation tandem mass spectrometry (RRLC-ESI-CID–MS/MS). Chromatography was conducted on a Zorbax SB C18 column (2.1 × 100 mm, 1.8 μm) at 30 °C, with a gradient mobile phase consisting of 0.05% formic acid and acetonitrile, a flow rate of 0.2 mL min^{-1}, and a total run time of 14 min. MS/MS acquisition parameters were as follows: positive ionization mode, dry gas: nitrogen, 10 L min^{-1}, dry temperature: 350 °C, nebulizer: 40 psi, capillary: −3500 V, scan range: 250–800. The autoMS, manual, or multiple reaction monitoring mode was selected as required. Two glucuronidated metabolites of puerarin (M1 and M2) were detected. M1 and M2 are presumed to be puerarin-7-*O*-glucuronide and puerarin-4′-*O*-glucuronide, respectively, and M2 likely is suspected to be the major metabolite because it represented the predominate peak. Kinetic studies of metabolites demonstrated that M1 and M2 were detected in rat plasma at 5 min after intravenous administration of puerarin, the levels of M1 and M2 then reached their peaks at 10–15 and 15–30 min, respectively. The metabolic profiles were similar in rat liver and intestine investigated by *in situ* liver and intestine perfusion, indicating that no metabolic regioselectivity of puerarin occurs in the two organs.

1. Introduction

Puerarin (7,4′-dihydroxyisoflavone-8β-glucopyranoside, Fig. 1a) is a major active ingredient of the traditional Chinese medicine Pueraria Radix, which comes from the kudzu root (*Pueraria lobota* (Willd) Ohwi). Puerarin has been widely prescribed for patients with cardiovascular diseases in China. It has been reported that puerarin exhibits comprehensive activities in the treatment of hypertension [1], arteriosclerosis [2], diabetes mellitus [3], and metabolic syndrome [4]. In addition, puerarin is a phytoestrogen, which is known to have dual biological functions: estrogenic activities and antiestrogenic activities [5].

In our previous pharmacokinetics study, we demonstrated that puerarin was distributed and eliminated rapidly when a single dose of puerarin was administrated (20 mg kg^{-1}) to rats intravenously. The $T_{1/2\alpha}$, $T_{1/2\beta}$ and Cl were 0.13 h, 1.06 h, and 0.10 L h^{-1}, respectively [6]. Although the level of puerarin in rat plasma and tissues was very low at 6 h post-dosing, the cumulative excretion rate of unchanged puerarin in urine and feces was 45.33% in 24 h [6,7]. Therefore, we speculated that in addition to the parent compound, metabolites of puerarin may have bioactivities that contribute to its pharmacological efficacy.

Investigating the metabolism of puerarin is essential to understand the underlying mechanism(s) for its therapeutic effects. However, only a few reports about the metabolism of puerarin are available [8–11], and high doses of puerarin were used in those studies. The present study focused on identifying the metabolites of puerarin and measuring their kinetics in plasma using rapid resolution liquid chromatography electrospray ionization-collision induced dissociation tandem mass spectrometry (RRLC-ESI-CID–MS/MS) after a single dose equivalent to the human clinical dose was given to rats intravenously.

A previous study reported that flavonoids were metabolized differently in liver and intestine [12]. In this work, the metabolites of puerarin in liver and intestine were identified and the metabolic profiles of the two organs were compared.

* Corresponding author. Tel.: +86 20 81340727; fax: +86 20 81340727.
E-mail address: gzminsheng@vip.163.com (M.-S. Chen).

1570-0232/$ – see front matter © 2009 Elsevier B.V. All rights reserved.
doi:10.1016/j.jchromb.2009.12.002

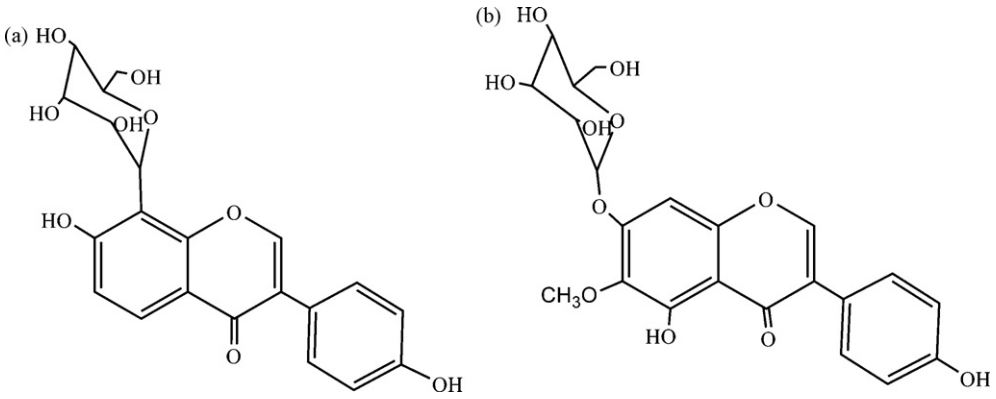

Fig. 1. Structures of puerarin and tectoridin. (a) Puerarin; mol. wt. 416; (b) tectoridin; mol. wt. 462.

2. Experimental

2.1. Chemicals and reagents

Puerarin and puerarin injection were purchased from Guangdong Greatsun Biochemical Pharmaceutical Co., Ltd. (Guangzhou, P.R. China). Both β-glucuronidase (type B-1, from bovine liver) and D-saccharic acid 1,4-lactone monohydrate were purchased from Sigma–Aldrich (St. Louis, MO, USA). Tectoridin (the internal standard, Fig. 1b) was obtained from the National Institute for the Control of Pharmaceutical and Biological Products (Beijing, P.R. China). Methanol and acetonitrile (HPLC grade) were purchased from Merck Chemical Ltd. (Darmstadt, Germany). Formic acid and acetic acid were purchased from Acros Organics (Geel, Belgium). Drug-free rat plasma was collected from healthy Sprague–Dawley rats of both sexes and stored at −20 °C. Ultrapure water was used throughout the experiments (Millipore, MA, USA).

2.2. Puerarin administration and sample collection

Specific-pathogen-free grade healthy Sprague–Dawley rats (180–220 g, 3 males and 3 females) were obtained from Guangdong Medical Laboratory Animal Center (Guangzhou, P.R. China). The rats were kept in an environmentally controlled breeding room (temperature 25 ± 2 °C, humidity 60 ± 5%, 12 h dark/light cycle) for 1 week before being used for the experiments. They were fed a soy-free custom diet (Guangdong Medical Laboratory Animal Center, Guangzhou, P.R. China) and water *ad libitum*. All animal handling and treatments followed the guidelines of the National Research Council. After overnight fasting, puerarin was intravenously administered (20 mg kg^{-1} body weight) via the jugular vein, and serial blood samples (approximate 0.3 mL) were obtained from the jugular vein at 0, 5, 10, 15, 30, 45, 60, 90, 120, 150, 180, 240, and 360 min post-dosing under pentobarbital sodium anesthesia (30 mg kg^{-1} body weight). Beginning at 1 h post-dosing, an equal volume of sterile physiological saline was injected after collection of each blood sample. Plasma was isolated by centrifugation of the blood at 13 000 rpm for 3 min. All samples were stored at −20 °C until analysis.

2.3. Sample preparation

Thawed plasma samples (100 μL) were placed in Eppendorf tubes. Next, 200 μL of a mixture of methanol and acetonitrile (90:10, v/v) was added to precipitate protein, and the samples were vortex mixed for 5 min and then centrifuged at 13 000 rpm for 10 min. The separated supernatant was centrifuged for 5 min at 13 000 rpm. Samples were analyzed immediately after preparation.

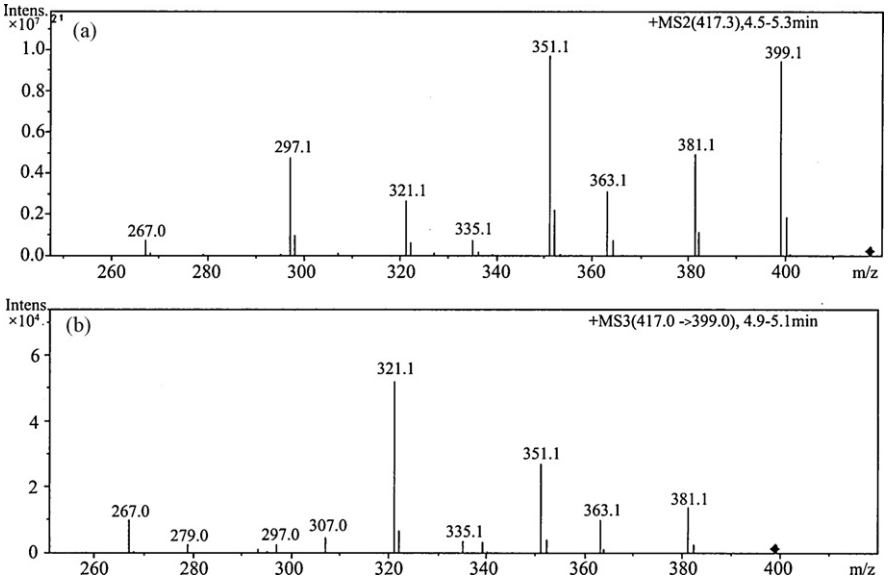

Fig. 2. Representative MS^n spectra of protonated puerarin (a: MS^2, b: MS^3).

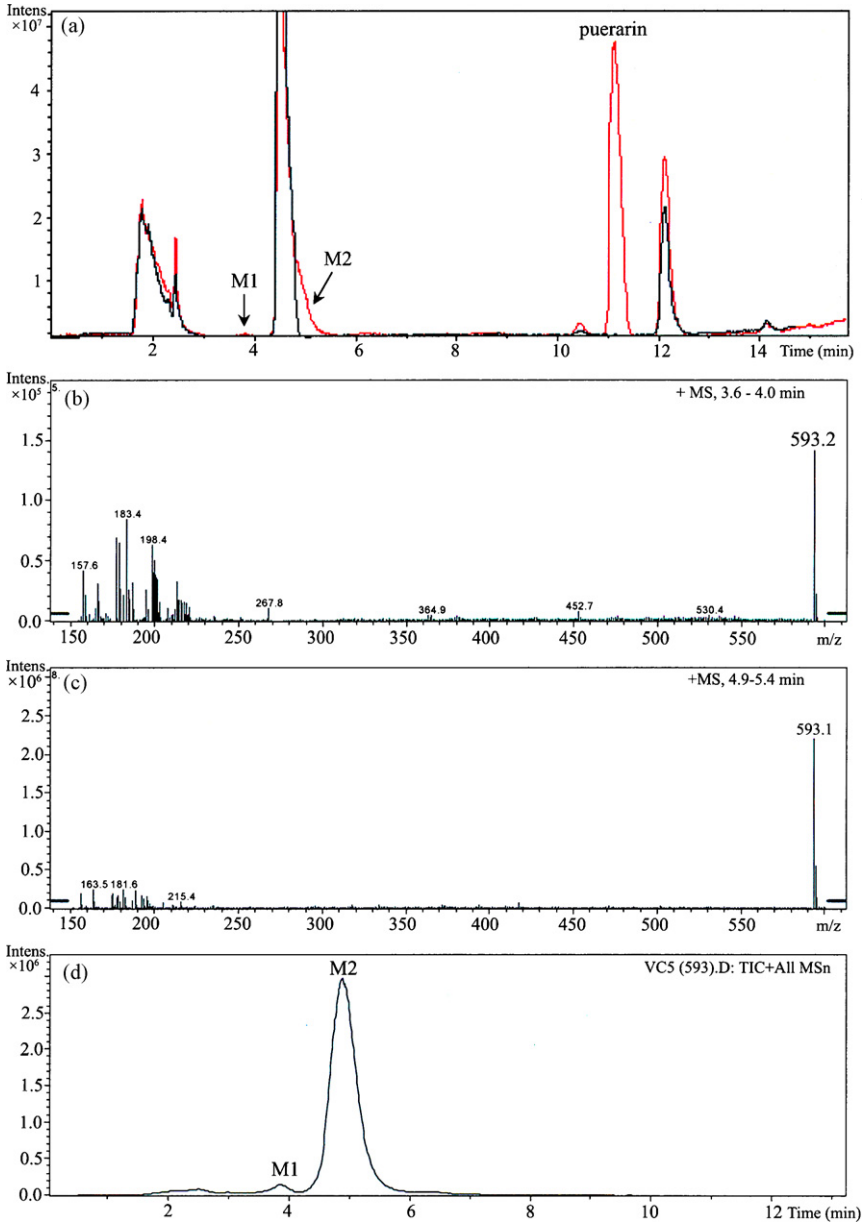

Fig. 3. Metabolites of puerarin in rat plasma. Two additional peaks were present in the TIC of rat plasma after puerarin administration (a, red profile). Both M1 and M2 showed the pseudo-molecular ion with a protonated molecule $[M+H]^+$ at m/z 593 (b and c), and the TIC of the same sample was detected in manual mode at m/z 593 (d). (For interpretation of the references to color in this figure legend, the reader is referred to the web version of the article.)

2.4. β-Glucuronidase reaction

To determine whether the metabolites could be hydrolyzed by β-glucuronidase, a 100 μL plasma sample was mixed with 100 μL water, 1 μL acetic acid, and 1 mL β-glucuronidase solution (1 mg mL^{-1}). To inhibit the activity of β-glucuronidase, a parallel sample was prepared, and 100 μL D-saccharic acid 1,4-lactone (11 mg mL^{-1}) was used instead of 100 μL water. The enzymatic hydrolysis was conducted at 37 °C for 24 h in the dark. To terminate the hydrolysis, 0.6 mL of methanol was added, and the mixture was centrifuged for 10 min at 13 000 rpm. The separated supernatant was analyzed immediately after preparation.

2.5. In situ rat liver perfusion

Krebs–Ringer buffer (118 mM NaCl, 4.8 mM KCl, 1.2 mM $MgCl_2$, 1.2 mM KH_2PO_4, 2.5 mM $CaCl_2$, 25 mM $NaHCO_3$ and 11 mM glucose) was used in perfusion experiments. The solutions were aerated with 95% O_2 + 5% CO_2, and maintained in a water bath at 37 °C.

The protocol for whole liver perfusion was modified based on the procedure reported by Inoue et al. [13]. The rats were anesthetized by intraperitoneal injection of pentobarbital sodium (30 mg kg^{-1} body weight), the abdomen was opened, and the liver, portal vein, and inferior vena cava were exposed. The portal vein was cannulated using a BD Intima-II integrated catheter (0.7 × 19 mm, Suzhou, P.R. China), and Krebs–Ringer buffer was pumped through the liver via the portal vein (0.3 mL min^{-1}). The subhepatic inferior vena cava was cannulated using a BD Intima-II integrated catheter. After the suprahepatic inferior vena cava and hepatic artery were ligated, the perfusion rate was set at 5 mL min^{-1} until the liver turned a khaki color; at this point, the puerarin buffer solution (0.5 mg mL^{-1}) was perfused and circulated at a constant rate of 0.5 ml min^{-1} for 1 h. The anesthetized rat was kept warm with an infrared lamp throughout the experiment. Finally, 0.5 mL

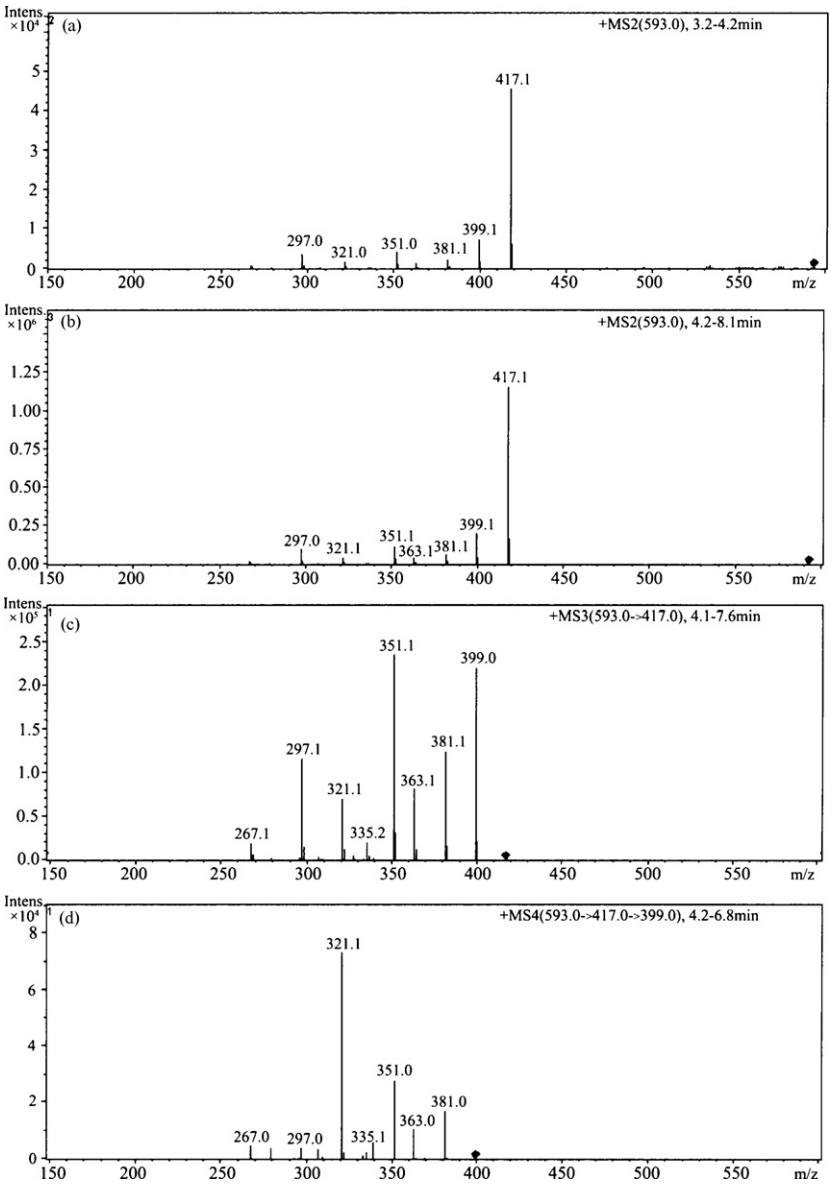

Fig. 4. MS^n spectra of M1 and M2. (a) MS^2 of M1 (m/z 593); (b) MS^2 of M2 (m/z 593); (c) MS^3 spectra of M1 and M2 (m/z 593 → m/z 417); (d) MS^4 spectra of M1 and M2 (m/z 593 → m/z 417 → m/z 399).

perfusate samples were centrifuged at 13 000 rpm for 5 min, and the separated supernatant was analyzed immediately after preparation.

2.6. In situ rat intestine perfusion

Rats were anesthetized by intraperitoneal injection of pentobarbital sodium (30 mg/kg body weight), the abdomen was opened, the abdominal aortic artery and kidney were exposed, and the kidney artery and celiac trunk were ligated. After the superior mesenteric artery and portal vein were cannulated using a BD Intima-II integrated catheter, respectively, the Krebs–Ringer buffer was pumped through the intestine at 5 mL min^{-1} until it turned a gray color, at this time, the puerarin buffer solution (0.5 mg mL^{-1}) was perfused and circulated at a constant rate of 0.5 mL min^{-1} for 1 h. The anesthetized rat was kept warm with an infrared lamp throughout the experiment. Finally, 0.5 mL perfusate samples were centrifuged at 13 000 rpm for 5 min, and the separated supernatant was analyzed immediately after preparation.

2.7. LC-ESI-CID–MS/MS analysis

LC-ESI-CID–MS/MS analyses were performed using an Agilent 1200 series rapid resolution liquid chromatography (RRLC) and a 6330 ion trap system consisting of a vacuum degasser, a binary pump, an autosampler, a column thermostat and a 6330 Ion Trap XCT Ultra mass spectrometer (MS) (Agilent Technologies, CA, USA). Chromatography was carried out on a Zorbax SB C18 reversed-phase column (2.1 × 100 mm, particle size 1.8 μm) (Agilent Technologies), proceeded by a guard column filled with C18 (Zorbax SB, particles size 1.8 μm). The injection volume was 5 μL. The column temperature was set at 30 °C. A gradient method was employed using 0.05% formic acid water solution as mobile phase A and acetonitrile as mobile phase B. For identification of metabolites of puerarin in rat plasma, the gradient started at 10% B and increased to 16% B over 6 min at a flow rate of 0.2 mL min^{-1}. For the kinetic study of metabolites and their enzymatic hydrolysis, the gradient started at 8% B and increased to 20% B over 10 min; over the next 2 min solvent B was increased from 35% to 65%, and the isocratic conditions lasted 3 min, The initial conditions were held

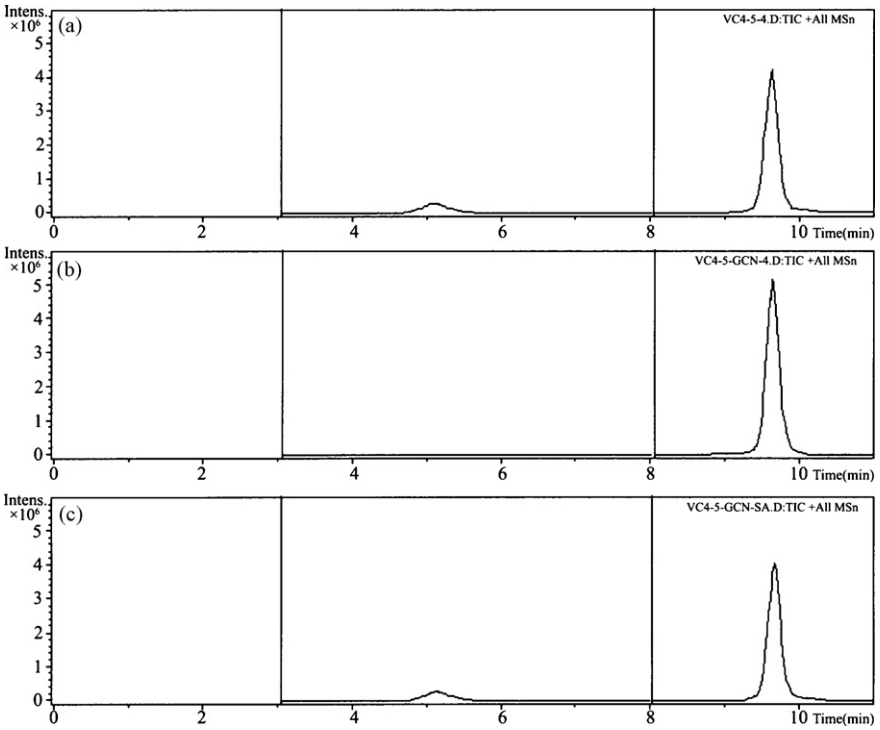

Fig. 5. TIC of plasma samples with or without enzymatic hydrolysis in the MRM mode (*m*/*z* 593/417, *m*/*z* 417/399). Puerarin glucuronides appeared in rat plasma after puerarin administration (a) and disappeared after the plasma represented in A was treated with β-glucuronidase (b); D-saccharic acid 1,4-lactone inhibited the enzymatic hydrolysis of β-glucuronidase (c).

for 8 min prior to the next injection, and a shorter Zorbax SB C18 reversed-phase column (2.1 × 50 mm, particle size 1.8 μm) (Agilent Technologies) was used due to a lower column pressure compared with a longer one.

The column effluent was introduced into the mass spectrometer, which was operated in electrospray ionization (ESI) positive ionization mode. Nitrogen was used as the nebulizing and drying gas at 350 °C, with a pressure of 40 psi and a flow rate of 10 L min^{-1}. The capillary voltage was set at −3500 V. The ion trap parameters followed the smart parameter setting, and the number of ion stored in the ion trap was controlled, with a target number of 500 000 and a maximum accumulation time of 200 ms. The scanning mass-to-charge (*m*/*z*) range was from 250 to 800 with a scanning speed of 26 000 *m*/*z* per second. For identification of metabolites of puerarin, the autoMS, manual or multiple reaction monitoring (MRM) mode was selected as required. For the kinetic study of metabolites and their enzymatic hydrolysis, MRM analysis was conducted by monitoring the precursor ion to product ion transitions from *m*/*z* 593/417 (puerarin glucuronides), 417/399 (puerarin) or 463/301 (tectoridin, internal standard). As the standards of metabolites were unavailable, the ratio of the peak area of the metabolite to that of the internal standard were used to determine the relative amount of individual metabolites in each plasma sample and to obtain a time profile for each metabolite. The RRLC and the MS system were controlled by Chemstation version B.01.03 SR2 and Ion Trap software 6.1, respectively.

3. Results

3.1. MS^n of puerarin

Fig. 2 shows the CID-MS/MS spectrum of the protonated molecule of puerarin. The MS^2 of the precursor ion at *m*/*z* 417 gave a series of product ions at *m*/*z* 399, 381, 363, 351, 335, 321, 297, and 279 (Fig. 2a). The MS^3 of the ion *m*/*z* 399 yielded a cluster of product ions at *m*/*z* 381, 363, 351, 335, 321, 307, 297, 279, and 267 (Fig. 2b). Our results are consistent with those of a previous report [14].

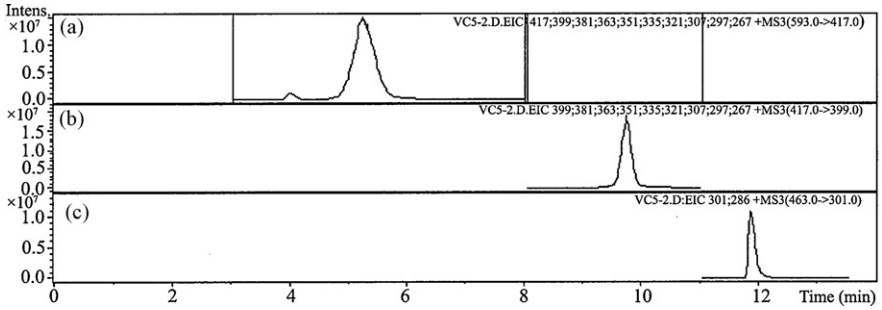

Fig. 6. Representative extracted ion chromatograms (EICs) of M1 (*m*/*z* 593 → 417) and M2 (*m*/*z* 593 → 417) (a), puerarin (*m*/*z* 417 → 399) (b), and the internal standard (tectoridin) (*m*/*z* 463 → 301) (c) in ESI positive ionization mode.

3.2. Metabolites of puerarin in rat plasma

To detect the metabolites of puerarin, the total ion chromatogram (TIC) of rat plasma after puerarin administration was compared to that of blank rat plasma. In addition to the puerarin peak, two peaks were found in the TIC of plasma of puerarin-treated rats, namely M1 and M2 in the order of elution (Fig. 3a). Interestingly, both M1 and M2 exhibited the pseudo-molecular ion with a protonated molecule $[M+H]^+$ at m/z 593 (Fig. 3b and c), although the peak of M1 was much smaller than that of M2 (Fig. 3d). MS/MS analysis of the ion at m/z 593 showed prominent product ions at m/z 417 (Fig. 4a and b) due to the loss of 176 amu. The MS^3 of the ion at m/z 417 yielded product ions at m/z 399, 381, 363, 351, 335, 321, 297, and 279 (Fig. 4c). The MS^4 of the ion m/z 399 yielded product ions at m/z 381, 363, 351, 335, 321, 307, 297, 279, and 267 (Fig. 4d). Taken together, M1 and M2 were considered to be puerarin-monoglucuronide isomers.

Incubation of the samples with β-glucuronidase resulted in complete elimination of the two metabolite peaks (M1 and M2) and a concomitant increase of the puerarin peak. D-Saccharic acid 1,4-lactone, an inhibitor of β-glucuronidase, inhibited the hydrolytic role of β-glucuronidase (Fig. 5). These results indicate that both metabolite peaks represented derivatives of glucuronidated puerarin.

Puerarin has two possible conjugation sites for glucuronidation: 7-OH and 4′-OH. It has been reported that 7-*O*-glucuronide was eluted prior to the elution of 4′-*O*-glucuronide during analysis by reversed-phase high performance liquid chromatography (HPLC) on a C18 or C8 column [15–17]. Our experiments demonstrated that the retention times for M1 and M2 were 3.9 and 5.0 min, respectively. Thus, we speculate that M1 and M2 are puerarin-7-*O*-glucuronide and puerarin-4′-*O*-glucuronide, and the latter may be the major metabolite of puerarin in rat plasma based on the peak area. The peak area ratio of M2 to the internal standard was at least 22 times that of M1 to the internal standard.

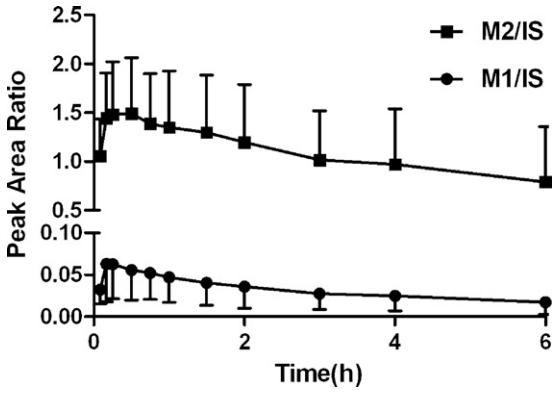

Fig. 7. Kinetics of metabolites of puerarin in plasma after single dose intravenous administration to rats (20 mg kg^{-1}, $n = 6$). M1, M2: metabolites of puerarin, IS: internal standard.

3.3. Kinetics of metabolites of puerarin in rat plasma

Prepared rat plasma samples were analyzed by RRLC-ESI-CID–MS/MS. M1, M2, puerarin, and tectoridin (the internal standard) were well separated under the gradient mobile phase, with retention times of 3.9, 5.2, 9.7, and 11.9 min, respectively (Fig. 6). To understand the kinetics of the metabolites in plasma after intravenous administration of puerarin (20 mg kg^{-1} body weight), the peak area ratios of M1 and M2 to the internal standard (tectoridin) were plotted against time. M1 and M2 were detected in rat plasma at 5 min after intravenous administration of puerarin, and the levels of M1 and M2 reached their peaks at 10–15 and 15–30 min, respectively. The levels of M1 and M2 declined subsequently, although the levels of M1 and M2 in plasma fluctuated (Fig. 7). These plots were intended to show only the relative metabolite levels, absolute quantification of the metabolites was not possible due to lack of the metabolite standards.

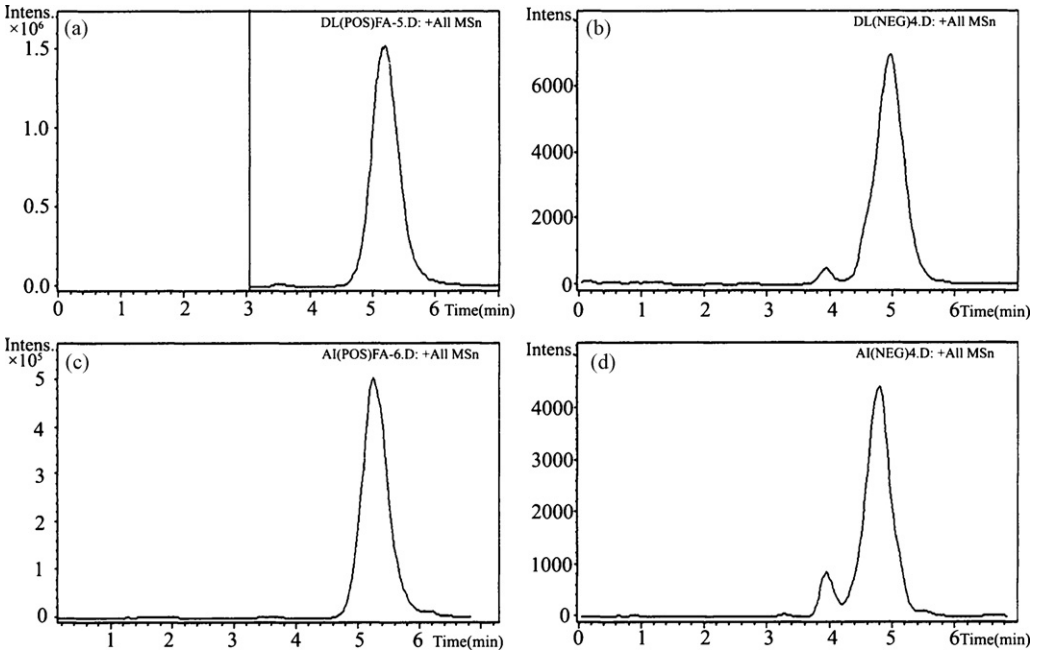

Fig. 8. Metabolites of puerarin in liver and intestine perfusate. Two glucuronidated metabolites of puerarin were appeared in the perfusate of liver (a) and intestine (c) when they were analyzed by LC-ESI-CID–MS/MS operated in positive ionization mode; similar profiles were obtained when the perfusate of liver (b) and intestine (d) were analyzed in negative ionization mode.

3.4. Metabolites of puerarin in perfusate of liver and intestine

To obtain and compare the metabolic profiles of puerarin in rat liver and intestine, puerarin was perfused through these organs. After 1 h of perfusion of the liver with Krebs–Ringer buffer containing 0.5 mg mL^{-1} puerarin, two glucuronidated metabolites appeared in the perfusate as determined with RRLC-ESI-CID–MS/MS (Fig. 8a); this finding indicated that a portion of puerarin was metabolized. The profile obtained from the liver showed high similarity with that obtained from plasma (Figs. 3d and 8a). The RRLC-ESI-CID–MS/MS operated in negative ionization mode (the mobile phase consisted of acetonitrile and 10 mM NH_4OAc in water, acetonitrile was increased from 8.5% to 16% over 8.5 min) was also used to analyze the same samples to determine whether a different profile would be obtained. A minor peak at 4.0 min (M1) and a major peak at 5.0 min (M2) were detected (Fig. 8b). Similar metabolic profiles were detected when the same sample was analyzed in positive ionization mode employing the identical mobile phase or a different mobile phase (acetonitrile–water containing 0.05% formic acid), although the detection sensitivity was greater in negative ionization mode. Similar metabolic profiles were obtained from the perfusate of the intestine (Fig. 8c and d).

4. Discussion

LC–MS has high sensitivity and selectivity, and multi-stage MS of each metabolite can provide abundant structural information. Thus this method has become a powerful tool for the identification of drug/chemical metabolites in biological materials. In this study, RRLC-ESI-CID–MS/MS was used to identify the metabolites of puerarin, the major active ingredient of Pueraria Radix.

Glucuronidation and sulfation are the major metabolic pathways for the disposition of flavonoids in humans and in experimental animals such as rodents. In the present study, two monoglucuronide conjugates of puerarin (M1 and M2) were detected in rat plasma when rats were administrated with puerarin intravenously, indicating that these glucuronides are the predominant metabolites of puerarin. Puerarin has two possible conjugation sites for glucuronidation: 7-OH and 4′-OH. It has been reported that different conjugation sites of the glucuronide group results in different retention behaviors in HPLC analysis [15–17]. An elution rule was reported when separation of flavonoid monoglucuronide isomers was performed by reversed-phase HPLC, that is, the 4′-glucuronide isoflavones were retained for longer than their 7-isomers [15–17], regardless of the exact chromatographic method employed. In our experiments, the retention times for M1 and M2 were 3.9 and 5.0 min, respectively, so that presumably, M1 is puerarin-7-*O*-glucuronide and M2 is puerarin-4′-*O*-glucuronide.

The content of M2 was much higher than that of M1 based on comparison of their peak areas in extracted ion chromatogram. Judging from the structure, it is not easy to glucuronidate at the 7-OH due to the presence of sterically hindered *C*-glucoside at the 8-position of puerarin [9]. In addition, it has been reported that the glucuronidation activity of 4′-OH is greater than that of 7-OH [18]. In our study, we observed that MS in negative ionization mode increased sensitivity for the detection of 7-glucuronide conjugates, which is in agreement with the results of Fang et al. [17]. However, the area of the peak that eluted later was much larger whether analyzed in positive mode or negative mode using the same mobile phase. Therefore, we conclude that M1 and M2 are puerarin-7-*O*-glucuronide and puerarin-4′-*O*-glucuronide, respectively, and that the latter is the major metabolite.

Prasain et al. [9] used MS operated in negative ionization mode to investigate the metabolism of puerarin in tissues of spontaneous hypertensive rats. They found that the area of the peak that eluted earlier was much larger than that of the later one. They considered the major peak eluting earlier to be puerarin-7-*O*-glucuronide and that eluting later to be puerarin-4′-*O*-glucuronide based on comparison of the relative retention times. Why our data and that of Prasain et al. [9] are inconsistent is unclear. The difference could be due to the different metabolisms of puerarin in tissues of spontaneous hypertensive rats and healthy rats. Further characterization of these conjugates based on NMR interpretation of standards is also required to reveal and confirm their exact structures.

Chen et al. [12] found that the 7-hydroxyl position appeared to be a main site for glucuronidation in rat liver. This scenario is quite different from that in the intestine [12]. In our study, similar glucuronidated metabolites (M1 and M2) were obtained in both liver and intestine perfusates; different metabolic profiles were not observed. In addition, M2 was considered to be the major metabolite in both liver and intestine perfusates. Thus, our results indicate that there is no positional difference of glucuronidation of puerarin between liver and intestine in healthy rats.

Flavonoids are absorbed into the plasma, and most of the absorbed flavonoids are present in the blood as conjugates [19] (e.g. glucuronide conjugates and sulfate conjugates). The fact that flavonoids exert biological effects in vivo in human intervention studies suggests that flavonoid conjugates may retain some biologically active properties. Indeed, some glucuronide conjugates have been shown to be active. For example, quercetin 4′-*O*-β-D-glucuronide and quercetin 7-*O*-β-D-glucuronide have antioxidant capacities [20,21]; a mixture of 5- and 7-*O*-β-D-glucuronide of hesperetin provided a 25% protection against ultraviolet-A-induced necrotic cell death; and baicalein 7-*O*-β-D-glucuronide inhibited the proliferation of DU145 cells [22]. Further pharmacological study of the functions of puerarin glucuronides is needed.

5. Conclusion

In summary, two glucuronidated metabolites (M1 and M2) were detected in rat plasma after a single intravenous dose of puerarin equivalent to the human clinical dose. These metabolites likely are puerarin-7-*O*-glucuronide (M1) and puerarin-4′-*O*-glucuronide (M2), respectively, and the latter might be the major metabolite (based on peak area). Similar metabolic profiles were found in liver and intestine perfusion experiments, indicating no metabolic regioselectivity of puerarin in rat liver and intestine.

Acknowledgements

Financial support for this research was provided by grant from the National High Technology Research and Development Program of China ("863" Program) (Grant number 2007AA022002) and the Guangzhou Science and Technology Bureau (Grant number 2007Z3-E5051).

References

[1] X.P. Song, P.P. Chen, X.S. Chai, Acta Pharmacol. Sin. 9 (1988) 55.
[2] L.P. Yan, S.W. Chan, A.S.C. Chan, S.L. Chen, X.J. Ma, H.X. Xu, Life Sci. 79 (2006) 324.
[3] F.L. Hsu, I.M. Liu, D.H. Kuo, W.C. Chen, H.C. Su, J.T. Cheng, J. Nat. Prod. 66 (2003) 788.
[4] M.E. Xu, S.Z. Xiao, Y.H. Sun, X.X. Zheng, O.Y. Yang, G. Chen, Life Sci. 77 (2005) 3183.
[5] C.S. Hwang, H.S. Kwak, H.J. Lim, S.H. Lee, Y.S. Kang, T.B. Choe, H.G. Hur, K.O. Han, J. Steroid Biochem. Mol. Biol. 101 (2006) 246.
[6] C.F. Luo, M. Yuan, M.S. Chen, S.M. Liu, L. Zhu, X.W. Liu, Lat. Am. J. Pharm. 28 (2009) 351.
[7] C.F. Luo, M. Yuan, M.S. Chen, W. Xiong, J. Tian, Strait Pharm. J. 21 (2009) 41.
[8] J.K. Prasain, K. Jones, N. Brissie, R. Moore, J.M. Wyss, S. Barnes, J. Agric. Food Chem. 52 (2004) 3708.

[9] J.K. Prasain, N. Peng, R. Moore, A. Arabshahi, S. Barnes, J.M. Wyss, Phytomedicine 16 (2009) 65.
[10] H.Z. Tian, B.C. Yang, J. Xu, H. Wang, Y.F. Guan, J. Sep. Sci. 29 (2006) 2692.
[11] T. Yasuda, Y. Kano, K. Saito, K. Ohsawa, Biol. Pharm. Bull. 18 (1995) 300.
[12] J. Chen, S. Wang, X. Jia, S. Bajimaya, H. Lin, V.H. Tam, M. Hu, Drug Metab. Dispos. 33 (2005) 1777.
[13] H. Inoue, H. Yokota, T. Makino, A. Yuasa, S. Kato, Drug Metab. Dispos. 29 (2001) 1084.
[14] H. Li, L. Wan, Y. Hashi, S. Chen, Rapid Commun. Mass Spectrom. 21 (2007) 2497.
[15] B.D. Davis, J.S. Brodbelt, J. Am. Soc. Mass Spectrom. 19 (2008) 246.
[16] B.D. Davis, P.W. Needs, P.A. Kroon, J.S. Brodbelt, J. Mass Spectrom. 41 (2006) 911.
[17] N. Fang, S. Yu, T.M. Badger, J. Agric. Food Chem. 50 (2002) 2700.
[18] L. Zhang, G. Lin, Z. Zuo, Life Sci. 78 (2006) 2772.
[19] H. Adlercreutz, H. Markkanen, S. Watanabe, Lancet 342 (1993) 1209.
[20] A.J. Day, Y. Bao, M.R. Morgan, G. Williamson, Free Radic. Biol. Med. 29 (2000) 1234.
[21] C. Morand, V. Crespy, C. Manach, C. Besson, C. Demigné, C. Rémésy, Am. J. Physiol. 275 (1998) R212.
[22] F.L. Chan, H.L. Choi, Z.Y. Chen, P.S. Chan, Y. Huang, Cancer Lett. 160 (2000) 219.